

# Variation in the Mechanical properties of Extruded Al-2099 after laser shock peening

Jige, Felix Teryima \*, Peter Ali Malgwi \*\*, Mohammed Isa Bappa \*\*\*

\* Department of Metalwork Technology, School of Technical Education, Federal College of Education (Technical), Potiskum., PMB 1013 Potiskum Yobe state, Nigeria

\*\* Metalwork Technology Department, School of Technical Education, FCE(T), Potiskum.

\*\*\* Metalwork Technology Department, School of Technical Education, FCE(T), Potiskum.

DOI: 10.29322/IJSRP.8.6.2018.p7820

<http://dx.doi.org/10.29322/IJSRP.8.6.2018.p7820>

**Abstract-** Laser shock peening (LSP) is an industrial process which creates rapid pressure rise in material surfaces giving rise to shock waves by using a high energy laser pulse. It offers 10 times increased life time as compared to the traditional mechanical shot peening.

In other to understand how strengthening precipitates are distributed in aluminum 2099 after been treated with Laser Shock Peening (LSP), hardness test was applied to an axially extruded T- shape of Al-2099. The result obtained from the hardness test showed variation in the hardness values of specimens extracted at different sections of the T shaped Al 2099.

The initial average hardness value of the flange was 140Hv while that of the web was 130 Hv. That was before laser shock peening was applied. After the application of laser shock peening, the initial softer part (Web) showed a higher value of hardness value of up to 170 Hv. The flange which was initially harder than the web before laser shock peening showed a hardness increment value of up to 160Hv. By implication, it means the softer web developed more residual stress meaning better response to laser shock peening.

The findings also showed that Al 2099 extruded T shaped exhibit different crystallographic textures at differing locations within the extruded cross section. This was reflected in the hardness variation. There was evidence of fibrous texture in the web and rolling texture in the flange.

Inhomogeneous texture showed influence on mechanical properties such as hardness value.

An average depth of laser shock penetration based on the peened condition for Al 2099 was recorded at 2 mm from the surface in to the material.

Approximately 18 % and 21 % increment in maximum surface hardness was recorded for the flange and web specimens respectively after treating them with Laser shock peening.

Hence, the users of software's solvers such as finite element analysis and eigen strain analysis for modelling should bear in mind the assumption of such geometry as continuum and assumption of homogeneous material properties and assumption of homogeneous material properties.

**Index Terms-** laser shock peening, Al 2099, Hardness, Mechanical peening, Mechanical properties, Compressive residual stress.

## I. INTRODUCTION

Aluminum alloys have a very wide application in the aviation industry most especially when it is alloyed with copper and lithium. This alloy has excellent specific strength (ESS) as well as corrosion resistant properties.

Compressive residual stresses (CRS) can be used to improve metallic fatigue life. Cyclic mean stress (CMS) is reduced thereby causing crack initiation difficult to initiate on the metal. This is followed with making the surfaces tensile to slow propagation of eventual cracks (Williams and Starke :2003).

Laser Shock Peening (LSP) is competitively used as a modern means of treatment of metals especially alloys. This is essentially done to improve on the mechanical properties of such alloys. In the aerospace industry where weight reduction with great functionality is the target, such treatments are important to achieve such target. In the aviation industry, the designed aircrafts are faced with cyclic, impact and static loads. Because of the environment in which it works, corrosion, erosion and cracks initiation are things to consider in the structural design. According to (Coratella: 2014), aircrafts are designed to withstand maximum load since the invention of the aviation industry in 1903. Cracks are due to imperfection of materials used in the design of airplanes. These cracks initiate and grow until they cause failure of the structural design of the airplane if not checked.

According to (Wanhill: 2003), most of the accident cases recorded in the aviation industry is because of cracks. He cited a case of the comet and the missing of F-111.

The designers of aircrafts design them in such a way that priority is given to safe life, safe failure and controlled failure. The safe life design consideration takes care of unpredictable crack by those parts of the aircrafts whose life span has reached. The controlled failure account for sensitive parts, designed to be structurally and strength wise reliable even after the effect of local failure. They controlled failure assume that cracks must develop during the service life of the aircrafts. Here, attention is paid to how these cracks can be controlled in such a way that they do not cause catastrophic failure by controlling their propagation properties.

Al-Li alloys have three important considerations that have made it candidate materials for the upper wings of aircrafts.

Lithium is the lightest metal. It reduces the aluminum density by approximately 3% weight with increased elastic modulus of approximately 6% for every weight percent (Xiao & Zhang, 2014) and (Williams & Starke, 2003).

The forming of the metastable  $\delta_1$  (Al<sub>3</sub>Li) phase which by appropriate thermal treatment can introduce precipitate hardening. The overall increase in specific elastic modulus and specific strength, attractive sub-surface microstructure and fatigue properties make Al-Li alloy attractive in the aerospace industry (Meriç, 2000). Related literatures on extrusion and effect of laser shock peening on mechanical properties and surface microstructure of 'T' shaped Al 2099 extruded will be critically reviewed.

**Influence of laser shock peening on mechanical properties & surface microstructure on extruded Aluminium 2099**

(Fitzpatrick et al., 2015), investigated the effect of laser shock peening on Al alloy 2634 in terms of hardening, state of heat treatment and crystallographic texture. Nanoindentation and incremental hole drilling was used to characterize the hardness and residual stresses of the specimens respectively. The extent to which laser shock peening parameters such as power density, spot size, peened layers and laser pulse duration on the depth, magnitude and uniformity of the introduced residual stresses and hardness on the material was investigated. Significant increase in hardness and residual stress was recorded by increasing the number of peened layers from 1 to 4 on Al 2634 in heat treatment state T351. The alloy in heat treatment state T39 however showed significant softness due to higher energies. 15% and 10% increase in hardness was recorded for the alloy in states T351 and T39 at 6GW/cm<sup>2</sup>. Generally, T3 is a designation assigned to solution heat treatment with cold working and natural aging to a reasonably stable condition. It is usually applied to cold worked products. The aim is to improve on the strength of the material after been solution heat treated (Kaufman, 2000) and (Kissell & Ferry, 2002). T39 and T351 are temper heat treatment designations for Al alloys. T3 stands for solution heat treatment with cold work and natural aging to a reasonable stable condition. 51 is a designation used for plate, rolled bars, forgings, die, extrusion or rolled rings that have undergone stress relief by means of stretching. 1 to 3 % are usually typical values of permanent set at the end of the stretching. No further treatment has been done after stretching (Campbell, 2011).

T39 stands for solution heat treatment. In this case, cold work has been done to degree that is appropriate to achieve the desired mechanical properties. In this case, cold working can be done before aging or after aging (Kaufman, 2000).

(Fitzpatrick et al., 2015), also investigated the texture of the alloy due to induced residual stresses by LSP. They recorded evidence of influenced preferred crystallographic orientation along the depth and magnitude of the introduced residual stresses. A plot of their tensile profile is shown in figure 1

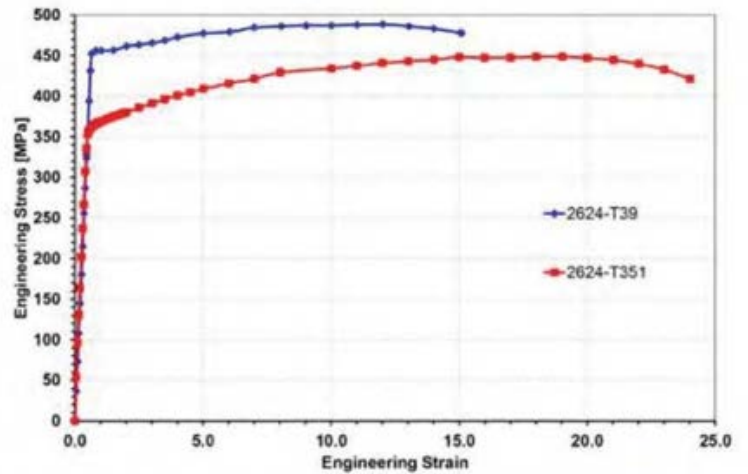


Figure 1: Tensile stress-strain profiles of Al alloys 2624-T39 and Al 2624-T351 (Fitzpatrick, et al., 2015) and the hardness profile is shown in figure 2.

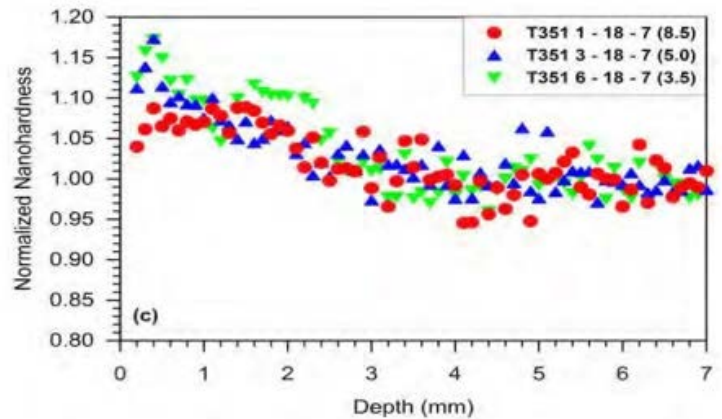


Figure 2: Normalised Hardness profile of Laser shock peened Al alloy 2624-T351 with the unpeened Al alloy 2624-T351 (Fitzpatrick, et al., 2015)

(Fitzpatrick et al., 2015), focused on the effect of laser shock peening on the microstructure based on the prior type of heat treatment given to Al-Li alloy especially when the LSP parameters are varied on Al-Li alloy.

(Sun et al., 2014) reported the use of shot peening as a surface treatment used to enhance the performance of metallic parts in automobile and aerospace industry. He concentrated on evolution of microstructure and mechanical properties of 2196 Al-Li. He measured the mechanical behavior due to shot peening of the surface using micro hardness. He used optical microscope to measure the microstructure of the shot peened specimens. The interesting thing about the study is the trend of the micro hardness he obtained after peening as shown in figure 3. However, the surface topography was distorted

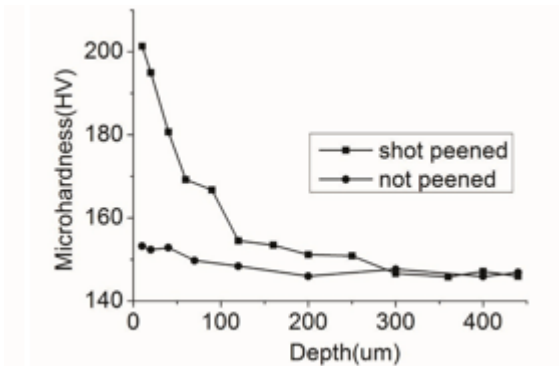


Figure 3: Micro hardness of unpeened and peened profile by (Sun et al., 2014)

In view of the promising result of peening as a surface treatment to aluminium and its alloys, the researcher was motivated to investigate specifically on Al 2099. Owing to the lighter nature of the alloy, it looks promising to save much weight as well as cost reduction should the findings prove positive.

In this research laser shock peening which has more advantages over the mechanical shot peening and which is a recent technology was used.

**Material description of Al-2099 alloy.**

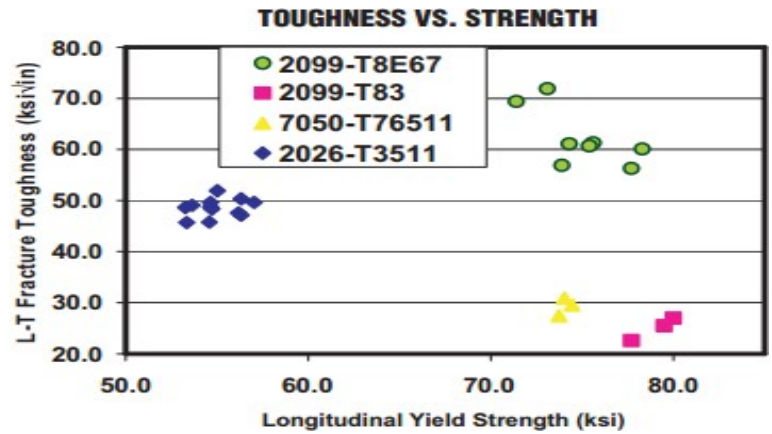
**Description**

Al-Cu-Li alloy or C460 developed by Alcoa has high strength, high stiffness, and excellent resistance to corrosion, superior tolerance to damage, weldability, and low density according to (Giummarra et al: 2007). More to that is the increase in modulus and strength with a corresponding reduction in density (Staiger et al: 2006).

These properties make al-2099 a choice in aerospace applications.

**Applications**

According to (Dursun and soutis: 2014), Al-2099 has better Mechanical properties than 2xxx, 6xxx and 7xx. It is



recommended for static and Fuselage structures with dynamic loading.

Good finishability for low manufacturing cost include good forming, surface finishing, fastening, and machining.

**Commercial status of Al-2099**

The commercial status of Al-2099 has been reported by (Giummarra et al: 2007) to have been commercially available in the mid-2000. He also, identified their specification on different Helicopters and commercial airplanes programmers. AMS 4287 has covered 2099-T83 and is included in MMPDS. MMPDS is reviewing 2099-T81 currently but it is covered by AMS 4459

**Toughness and fatigue of Al-2099**

According to (Dursun and soutis: 2014), there is an improvement in the S/N fatigue and crack resistance. It has improved performance over the previous 2024-T3511 critical fatigue standard for product applications.

Figure 4: Toughness vs strength of AL-2099 (Kramer et al: 2002)

A graph of Al-2099 toughness vs Strength is shown in Figure.

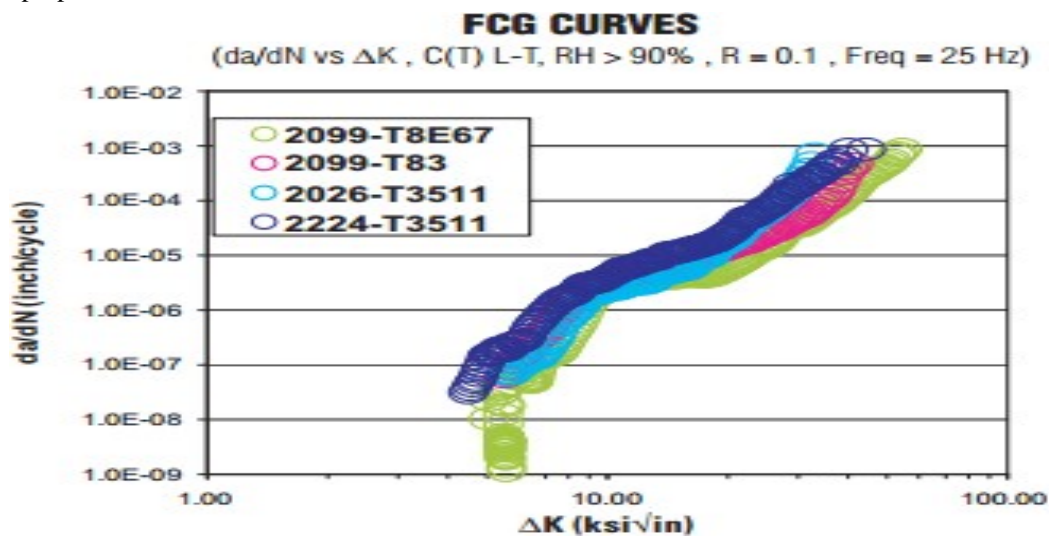


Figure 5: FCG Curves (Prasad et al., 2013)

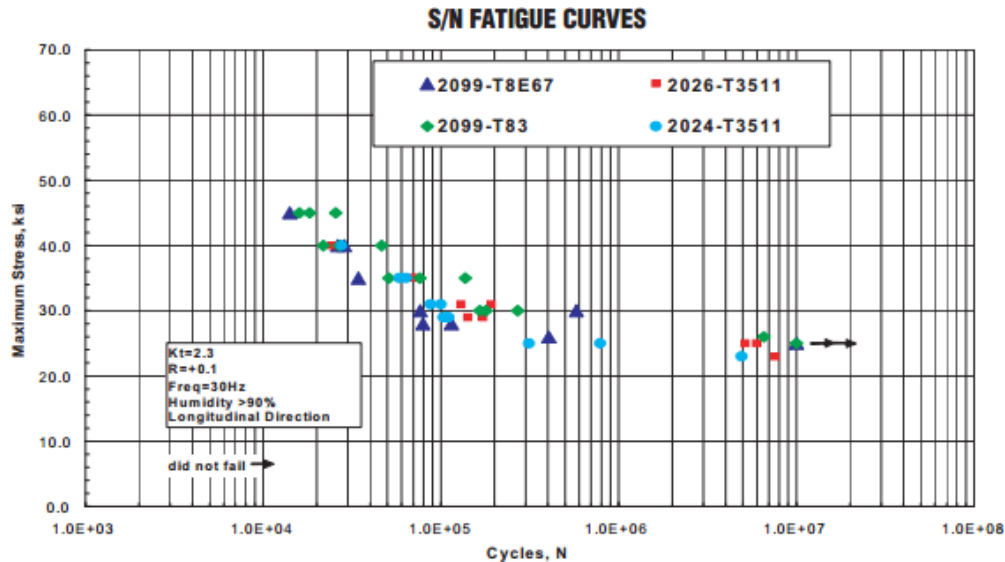


Figure 7: S/N fatigue curves (Giummarra et al: 2008)

**Corrosion resistance of Al-2099**

Compared to 2024-T3511 and 7075-T6511, Al-2099 offer higher resistance to corrosion (Liu: 2006). The T83 and T8E67 have better exfoliation rating than conventional alloys (Kramer: 2002). There is improved stretch—corrosion performance with long transverse ratings/ ASTMG64 of “A” when compared with the conventional “B” and “C” (Liu et al: 2015).

**Performance at elevated temperature**

According to (Srivatsan et al: 2013) and (Giummarra et al: 2012) both have reported that the Al 2099 of tempered T81 and T83 show improvement over the 2219 aluminium alloys. This improvement makes it candidate materials for applications at elevated temperatures.

**Method (Experiment)**

Hardness test measures material resistance to indentation. Hardness testing methods and specifications include the list; Rockwell – ASTM E18; NASM- 1312-6, Superficial Rockwell – ASTM E18; NASM-1312-6, Brinell – ASTM E10, Microhardness – ASTM E384; NASM-1312-6, Vickers – ASTM E384, ASTM E92, Shore – ASTM E2240. The Brinell test has a wide application to metallic materials. It is also the most commonly used test for cast and forged metals.

**Description of specimens for hardness test**

Laser shock peened specimens were used for hardness test in this study. The specimens were sectioned along the drilled hole, grounded and polished for hardness test. The specimens measured 25× 15 × 10 mm<sup>3</sup>. The unpeened specimens were treated in like manner. Details of shock peening parameters and the locations the specimens were extracted is shown in table 2.

Table 1: Al 2099 with one spot peening condition

Specimen label	Machined position	Orientation	Peened condition Power density/pulse duration/number of shots (GW/cm <sup>2</sup> -ns-#)	Spot Size/ mm <sup>2</sup>	Hole Depth
1a	Flange location	YZ	3-18-1	4	1.4
2a	Flange location	XY	3-18-1	4	1.4

4a	Web location	XY	3-18-1	4	1.4
5a	Web location	ZX	3-18-1	4	1.4
6a	Web location	YZ	3-18-1	4	1.4
12a	Web Location	XY	3-18-1	4	1.4
20a	flange location	YZ	3-18-1	4	1.4

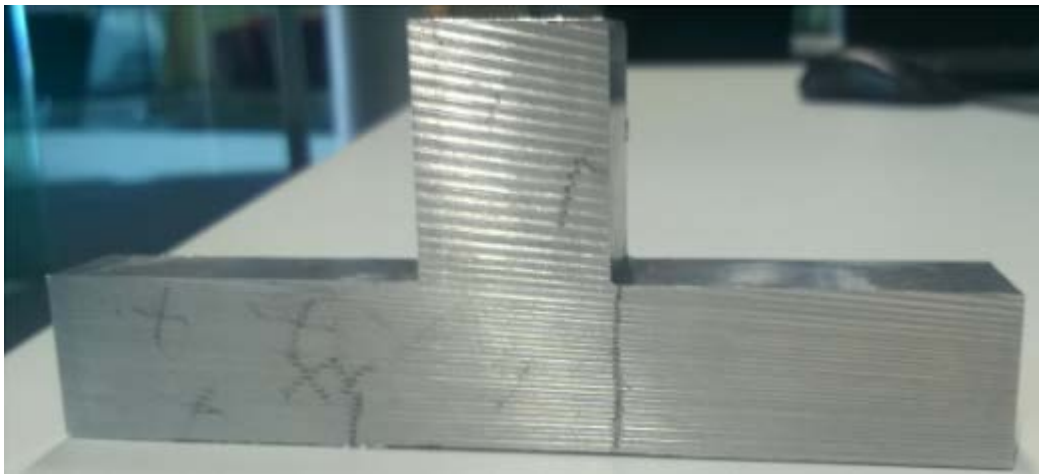


*Figure 4: Camera picture of extruded Al 2099 as received.*

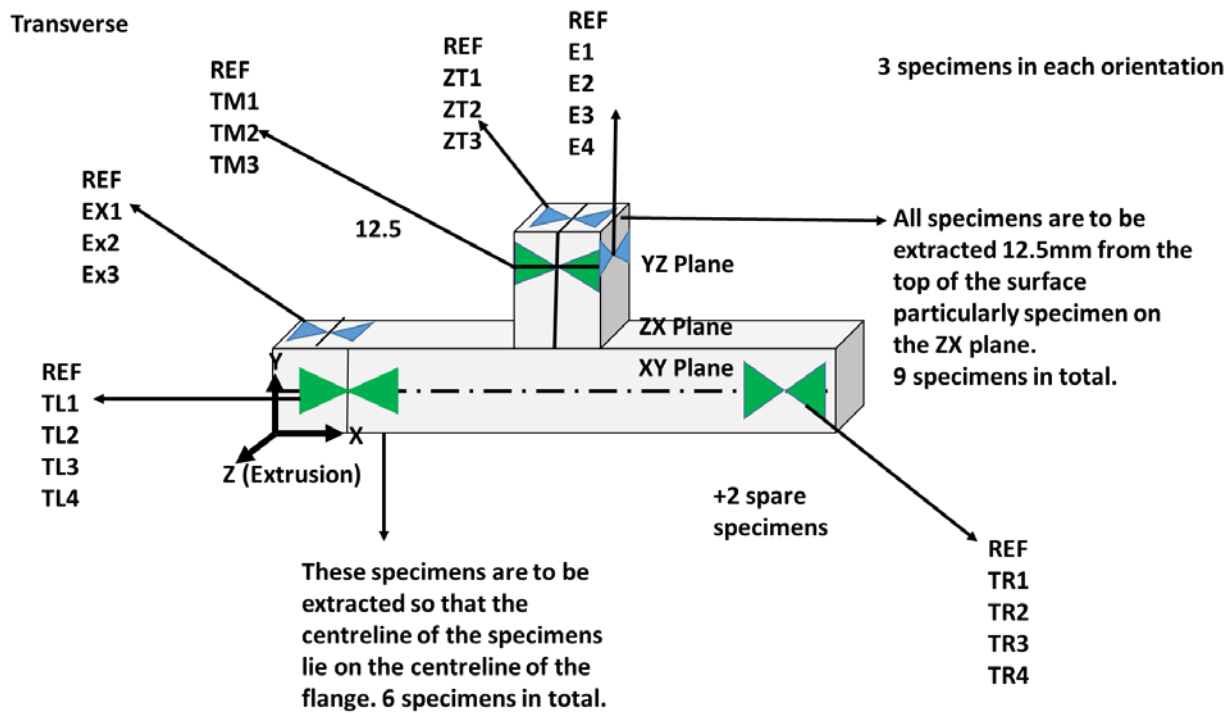


Figure 5: Positions of extracted specimens for tensile test

The specimens were marked and sectioned in the middle in the middle of the drilled hole as shown in figures 10 and 11 respectively.

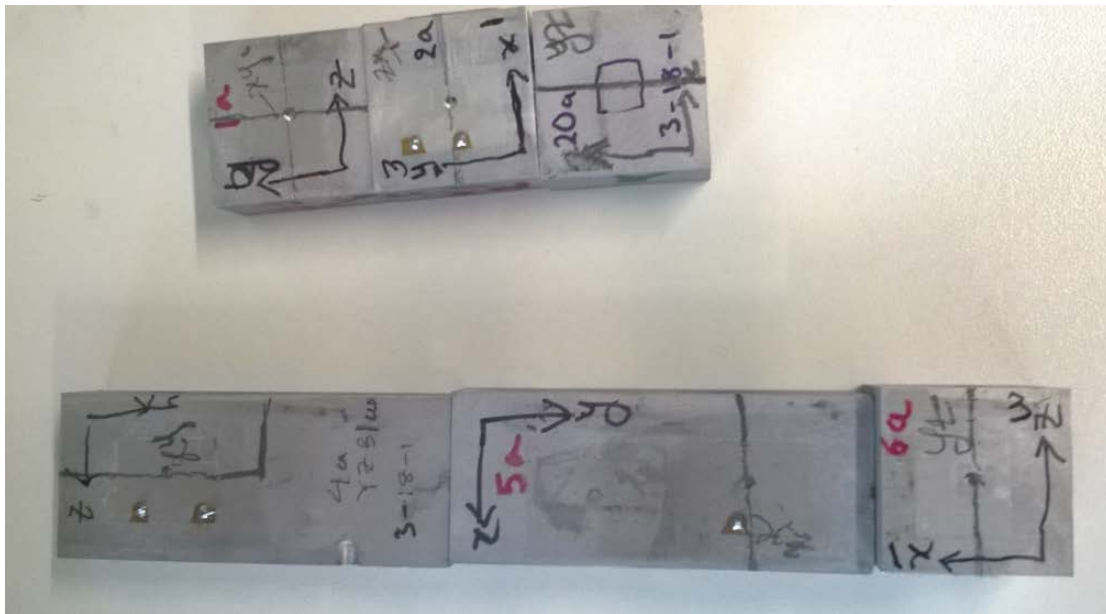


Figure 6:: Unsplitted LSP Labelled specimens of Al 2099 for harness test showing the position of the peen and hole.

Specimens of aluminium were treated by Laser shock peening. The area of treatment covered  $4\text{mm}^2$ . After the peening the specimens were splitted along the centre of a hole drilled in the middle of the peened area as shown in figure 10.



*Figure 7: Al 2099 specimens for hardness test marked and sectioned along the drilled hole.*

### **Preparation of specimens for hardness and analysis of Al 2099**

Sample preparation is the way a sample is treated or handled before data is obtained from it. Different measurement requirements require different preparation techniques. The way a sample is placed, sectioned, grounded and polished for obtaining data amounts to sample preparation.

Because of Aluminium's soft nature, care should be taken while preparing the sample for hardness and tensile test. It is however not sensitive to neuman bands or mechanical twins like Titanium and Magnesium. Neumann bands or Neumann lines are fine patterns of parallel lines usually seen in cross sections of iron meteorites. They are seen after polishing and treating the meteorite cross section with acid. Al has good corrosion resistance properties. The thin oxide film on the polished surface makes etching difficult.

The following steps were used for metallographic preparation; Sectioning, mounting, grinding and polishing. The steps highlighted by (Kalka & Adamiec, 2006), are discussed in detail.

### **Sectioning**

Sectioning is a standard cutting technique used in cutting materials. Different sectioning procedures may cause different surface damages depending on the type of sectioning procedure used. It is required to use the correct cutting blade or wheel, right cooling, controlled feed and pressure. Large diameter cutting wheels require minimum thickness for lower surface damage and good surface finish. The temperature of all cutting procedures should be minimum to avoid alteration of the alloy microstructure and hardness.

The cutting machine used in this study was Struers. After sectioning, the samples were ready for mounting.

### **Grinding**

Automated Motopol 2000 Struer machine, was used for the grinding of the unmounted samples. Different sizes of silicon carbides were used. 600-grit (rough silicon) was used followed with smooth silicon carbide.

Grinding of the sample was performed on the Automated Motopol 2000 Struer Machine as shown in figure 12 with a 600 grit Emery paper. The sample was rotated gently on the surface of the Emery paper placed on the automated rotating plate of Automated Motopol 2000 Struer machine until circular lines were



*Figure 8: Motopol 2000 Struer auto polishing machine for metallographic preparation.*

### **Polishing**

Polishing is the act of rubbing the Al surface on a diamond Abrasive to make it mirror shiny. The polisher does it by removing the scratches on the surface of the Al-alloy. The polishing Of the specimens were done with diamond suspension to polish between 6 to 1 microns. Polishing lubricant was used to avoid the precipitation of the polishing liquids.

The sample was placed at the pot edge such that slight runs out were obtained as the platen rotates along with the polish cloth. This was done to reduce differential polishing and edge retention. The polishing was done using the following steps;

1. The specimens were grounded with 240 grit water proof silicon paper at 200 rpm. A light force was applied on the specimen holder. There was a complementary platen and holder rotation in the same direction. The samples were washed, rinsed and dried when the surfaces became co-planar.
2. A 9 $\mu$ m Diamond polish paste was used on a silk MD-Dur with a green lubricant to avoid precipitation of the paste. A speed of 120-150rpm was used to with a load of about 23N per sample in complementary rotation.

The polish slurry was squirted in an interval 2mins to refresh the surface. The lubricant was added in 30s cycle intervals. The sample were washed, rinsed in water and blown dry with compressed air.

3. The polishing was followed with a 6 $\mu$ m polish paste on MD-Sat Pad for 3mins circle time as in step 2 manner wise.

4. 1 $\mu$  Diamond polish paste was used to remove the light scratches using MD-Sat pad as in steps 2 and 3 for 2mins circle time.
5. This step required a MD-Chem pad, MD-Floc or colloidal Silica at a speed of 120-150rpm at 120s. A force of 23N was applied per sample while rotating in the contra direction. The sample was washed, rinsed and blown dry with compressed air as shown in figure 13.

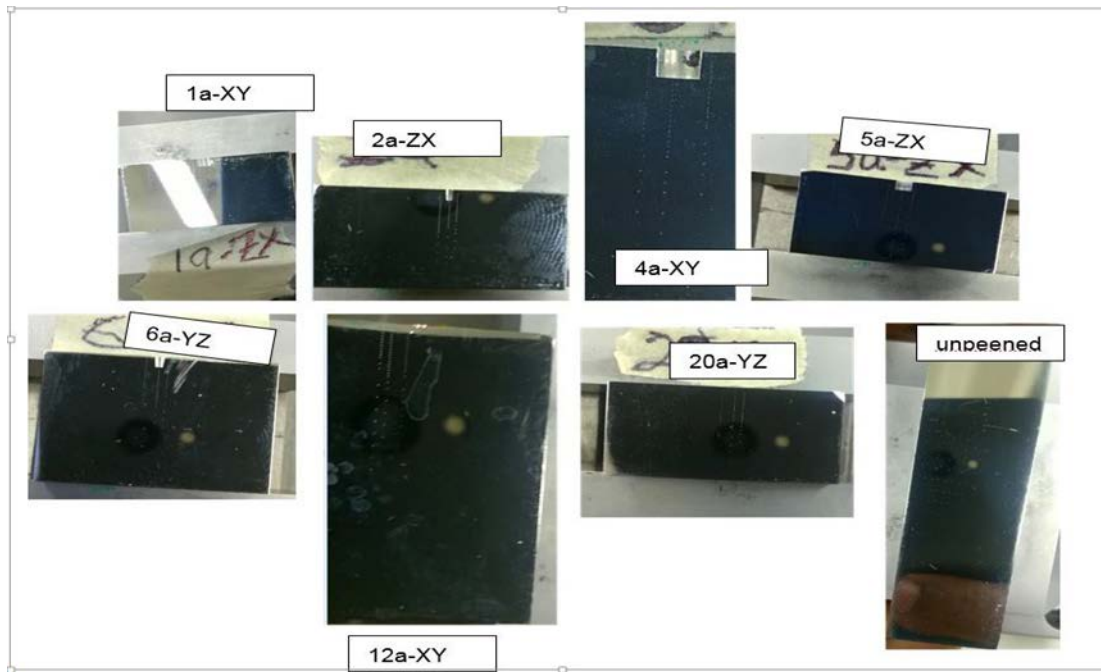


**Figure 9: Prepared specimens for indentation.**

### Hardness test description

Solid materials generally exhibit three changes viz; elastic, plastic, and fracture changes when stressed. The strong intermolecular forces in the hard materials allow them to withstand external forces without changing their shape permanently (Schuh et al., 2007).

Hardness test is carried out to understand the complex behavior of force on a solid matter (Cohen et al., 1998). Types of hardness test include indentation, scratch and rebound hardness (Chandler, 1999). In this work, the researcher used Vickers indentation hardness test.

Hardness test measures material resistance to indentation. Hardness testing methods and specifications include the list; Rockwell – ASTM E18; NASM-1312-6, Superficial Rockwell – ASTM E18; NASM-1312-6, Brinell – ASTM E10, Microhardness – ASTM E384; NASM-1312-6, Vickers – ASTM E384, ASTM E92, Shore – ASTM E2240.

Vickers Hardness test can be used to test different materials irrespective of their hardness. The ease of use makes it a choice of many. It observes the materials resistivity to plastic deformation from standard source. It can test all metals including aluminum. This method is used because of the ease of use of the machine, it is relatively inexpensive, little practice is required, and the specimens will not be destroyed at the end of test. In this study, the hardness test used was Vickers hardness test because the measurement indents starting from the peened surface and

from the middle of the drilled hole. After 4 mm, the spacing changed to 0.5mm between indents. From 5mm, the spacing between indents changed to 1mm. 16 indents were made in the first 4mm. the remaining indents were spread out along the width of the specimen. All procedures were according to ASTM, 2002 tensile testing standard. is only meant for comparison of the effect of shock peening along the radius area and depth of the peen compared with the unpeened specimen. Specimens of aluminum were treated with Laser shock peening.

The peened area was 4mm<sup>2</sup> with a 1.4 mm hole drilled in the middle of the peened area. After the peening the specimens were splitted along the center of a hole drilled in the middle of the peened area.

Cut specimens were metallographically prepared for hardness test. Hardness test was performed using MVK-H1 Mitutoyo Hardness Testing Machine. The test was performed with a spacing of 0.25mm between A total of three sets of indents were made for each specimen with 0.5 mm before the hole, mid-way under the hole and 1 mm after the hole. The MVK-H1 Mitutoyo Hardness Testing Machine was used for the test.

Precautions were adhered to while performing the hardness test. Laboratory coat was worn while carrying out laboratory test. The zero mark was prechecked and set at the beginning of new test. The polished specimens ready for hardness test are shown in figure 14.



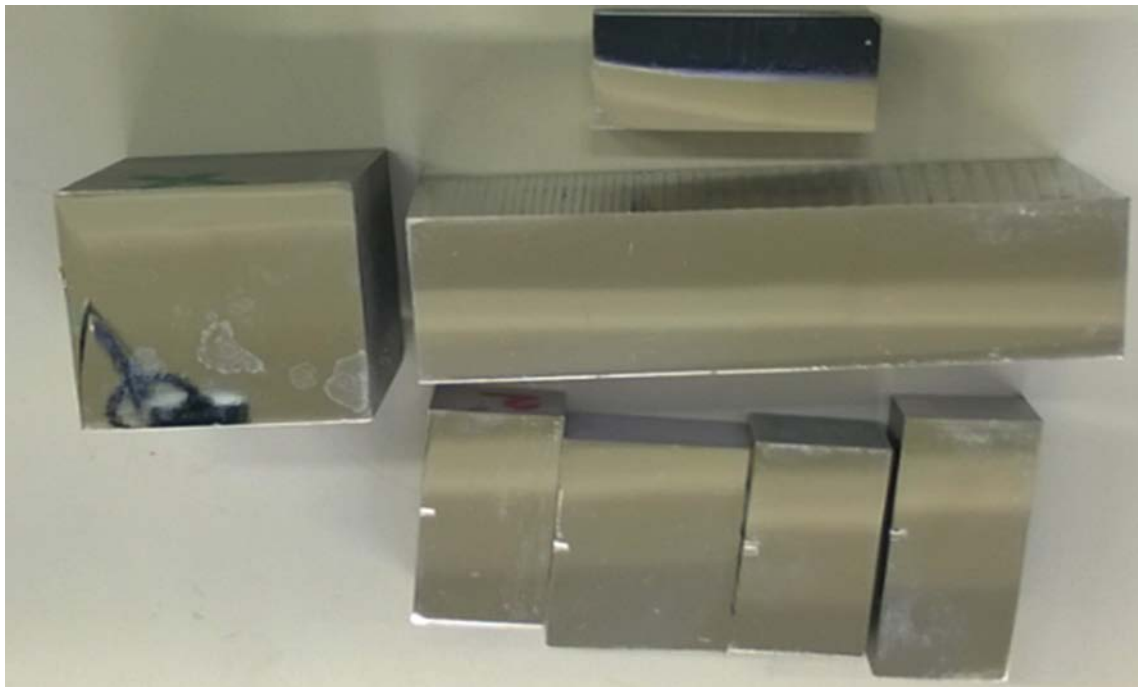


Figure 10: Polished specimens ready for hardness test.

The marked position shown in figure was applied on the specimens in figure 15.

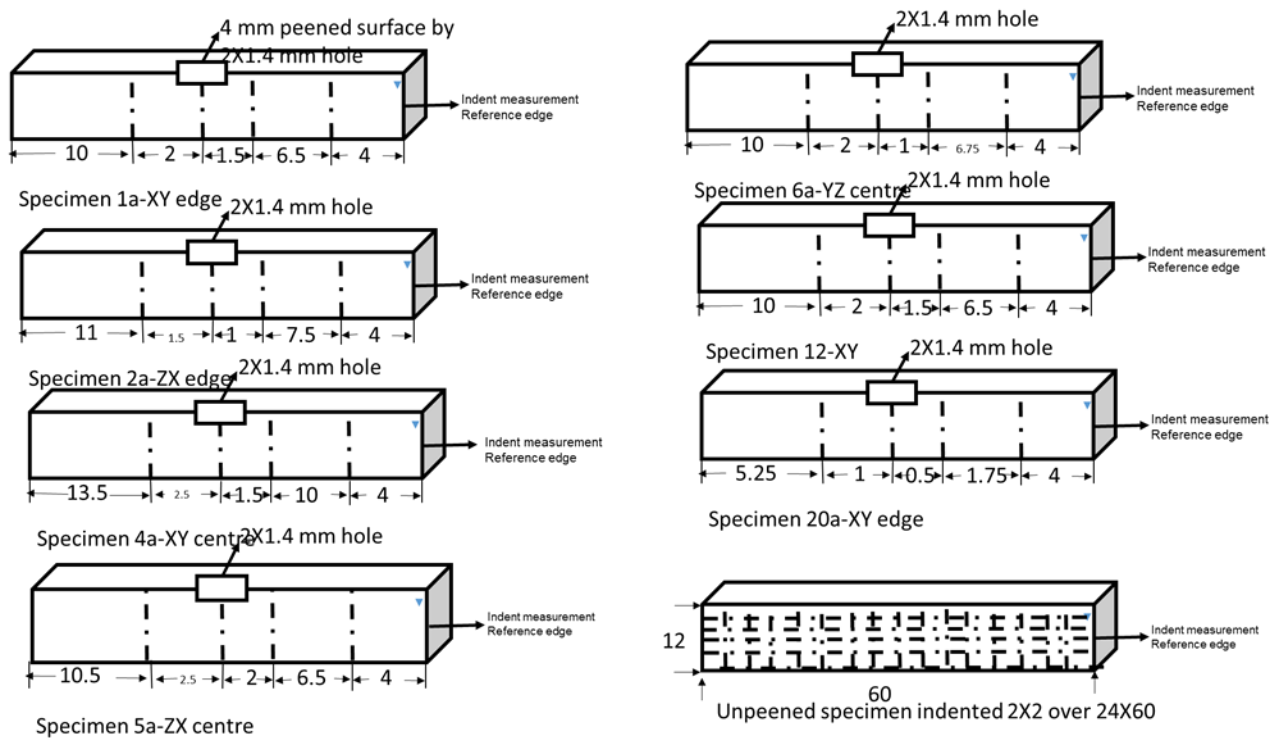


Figure 11: Schematic diagram of the indented specimens

Vickers Micro hardness also uses the pyramid shape diamond with an exact defined force to create an indent on the specimen. The surface area is measured and evaluated in mm squares. Mathematically, Vickers hardness  $HV = \text{Test Force } F \text{ divided by the surface area of the indentation}$

(Olivier et al., 2008). The surface area (SA) of the pyramid Diamond Head based for indenting is given by  $S^2 + 2(S*L)$ . The hardness value relationship is shown in figures 20 and 19.

$$H_{IT} = \frac{F}{A_P \cdot h_c^2} \quad A_P = 23.96$$

Figure 12: Hardness value relationship (Olivier et al: 2008).

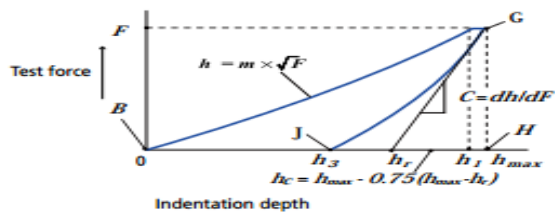


Figure 13: Hardness test (Wang et al., 2003)

where L is the slant height of the triangles and S is the base square side length. Hardness test is performed to characterize surface hardness (Fischer, 2000). A load of 50N was applied to the Specimens of Al-2099 for a period of 10 seconds. The surface area of the indent created was then measured and the data got was plotted as Hardness vs Position from peened surface. Hardness Test Result and Discussion

The result obtained from the hardness test of specimens extracted as shown in figure 26

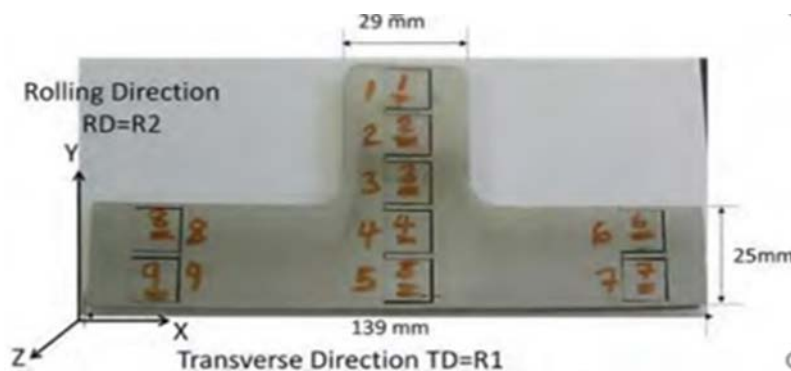


Figure 14: positions of peened specimens as extracted on the T shape (Fitzpatrick et al., 2015)

are shown in figures 19 to 24. From the result, it clear that Al 2099 responded to the peened condition presented in table 4. There was a 21% increase in the maximum surface hardness values of the peened specimens in the web and 18% increase in the maximum surface hardness values of the peened specimens in the flange as compared with the unpeened specimen.

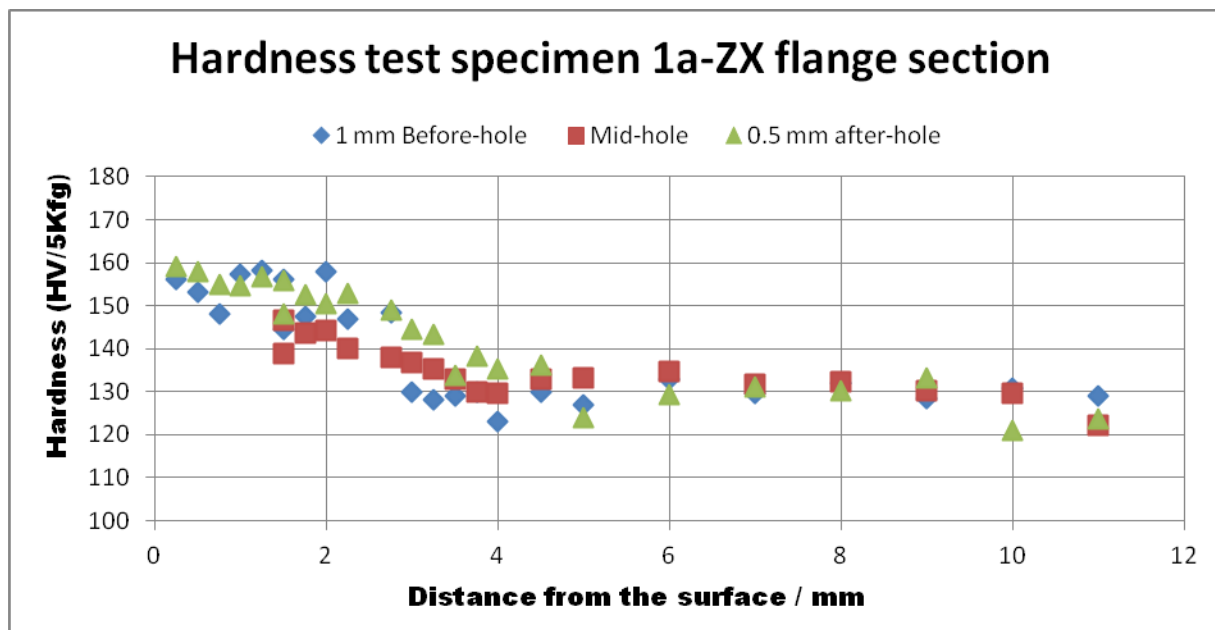


Figure 15: Result of hardness test on laser shock peened specimen 1a in the flange section of Al 2099.

The highest surface hardness value of specimen 1a is approximately 160 Hv. The depth of the effect is approximately 2mm. The average hardness value of the unpeened section is 135 Hv to 140 Hv.

Worthy to note is the fact that the measurement directly under the hole do not have values 1.4 mm length. This is because, the measurement started 1.4 mm into the specimen. The same will be observed on the rest of the specimens.

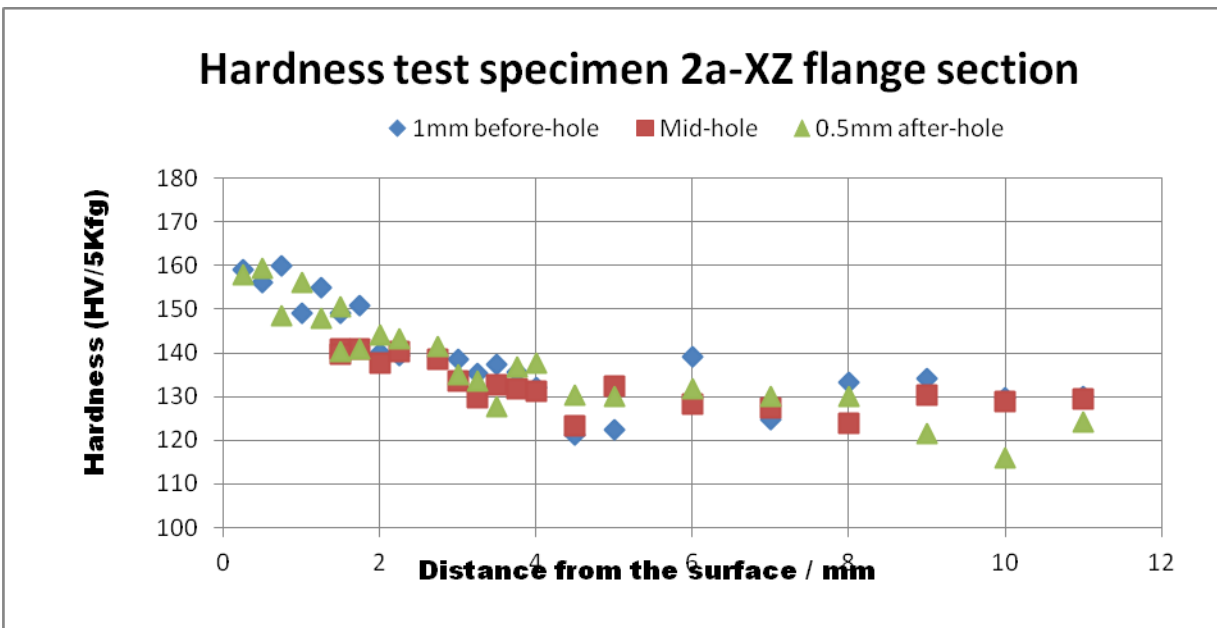


Figure 16: Result of hardness test on laser shock peened specimen 2a in the flange section of Al 2099.

The approximate highest value of specimen 2a extracted from the flange is 160 Hv still. The average effective laser shock peening depth is 2 mm into the specimen. The average hardness value outside the peening effect is scattered between 130 Hv to 140 Hv.

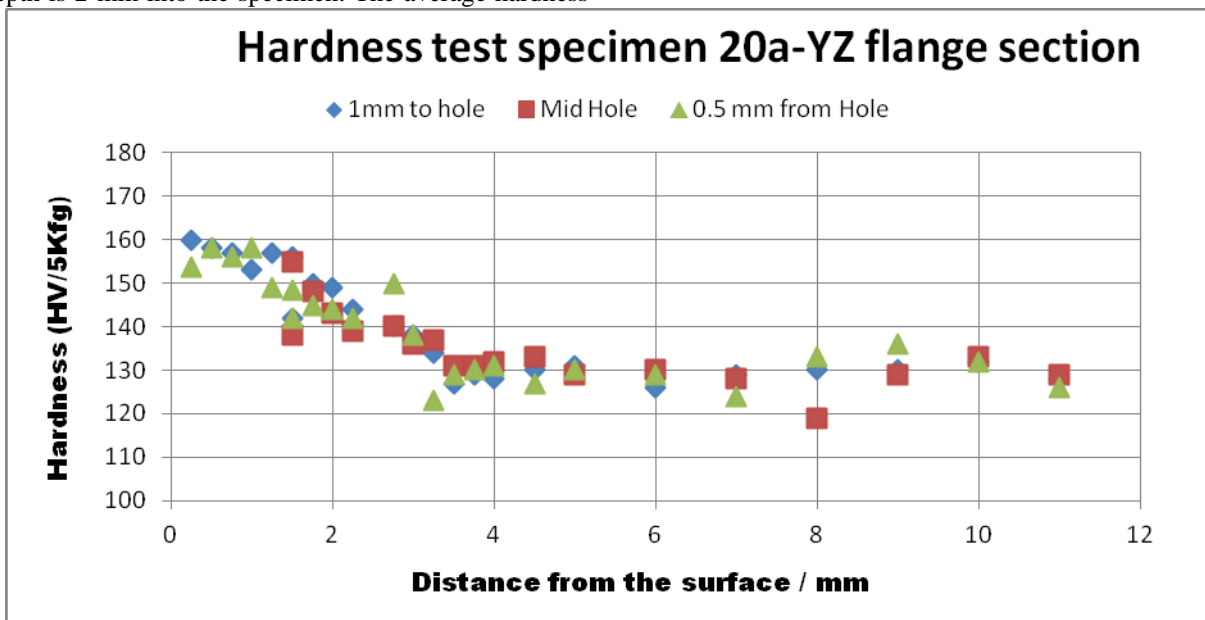


Figure 17: Result of hardness test on laser shock peened specimen 20a in the flange section of Al 2099.

Specimen 20 a shows average maximum surface hardness value of below 160Hv. The average hardness value outside the peened effect is scattered between 130 Hv to 140 Hv. Effective depth of peening is approximately 2 mm.

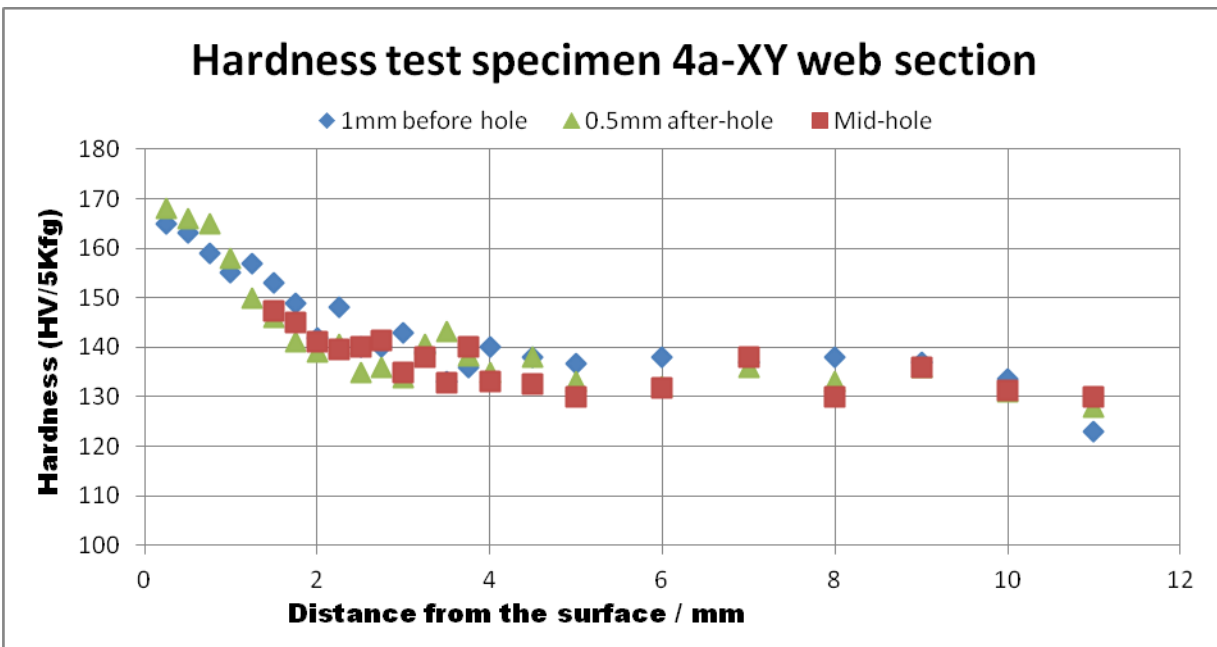


Figure 18: Result of hardness test on laser shock peened specimen 4a in the web section of Al 2099.

The specimens in the web section showed a higher maximum hardness value of approximately 170 Hv as compared with 160 Hv maximum surface hardness value obtained from specimens in the flange section. The effective depth of peening is

about 2 mm but with less scatter values. The range of hardness values outside the peening effect is between 130 Hv to 140 Hv.

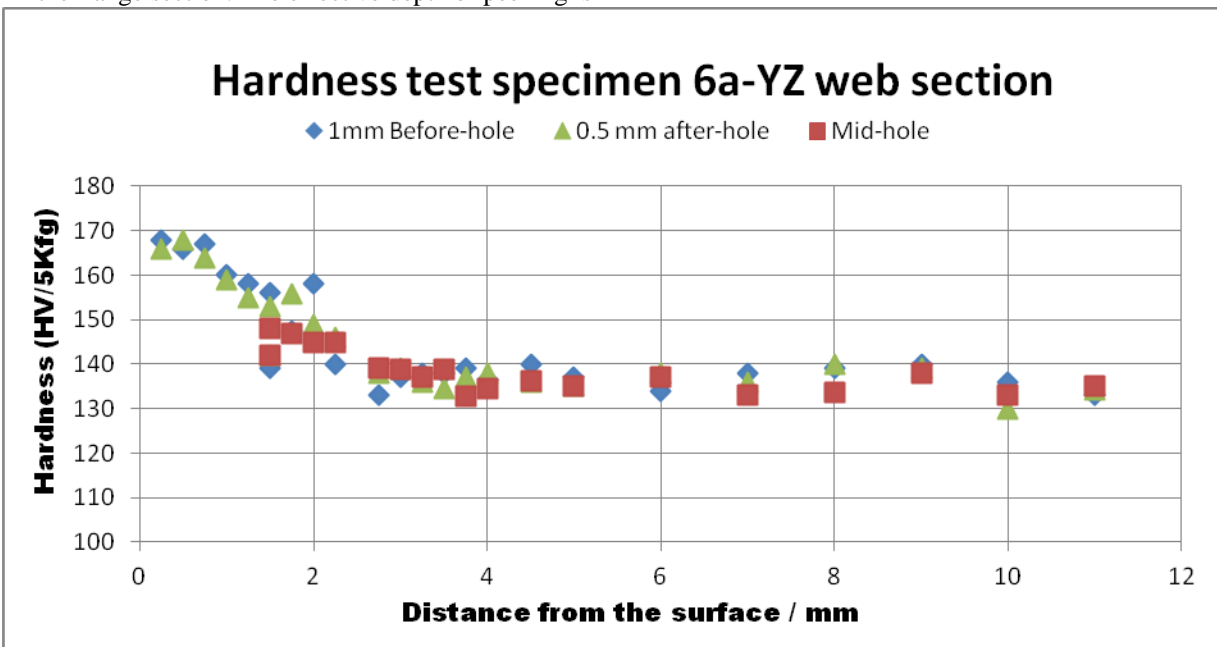


Figure 19: Result of hardness test on laser shock peened specimen 6a in the web section of Al 2099.

Approximate maximum surface hardness value due to laser shock peening is approximately 170 Hv. Effective depth is

approximately 2 mm. unpeened section measures average hardness value of 130 to 135 Hv.

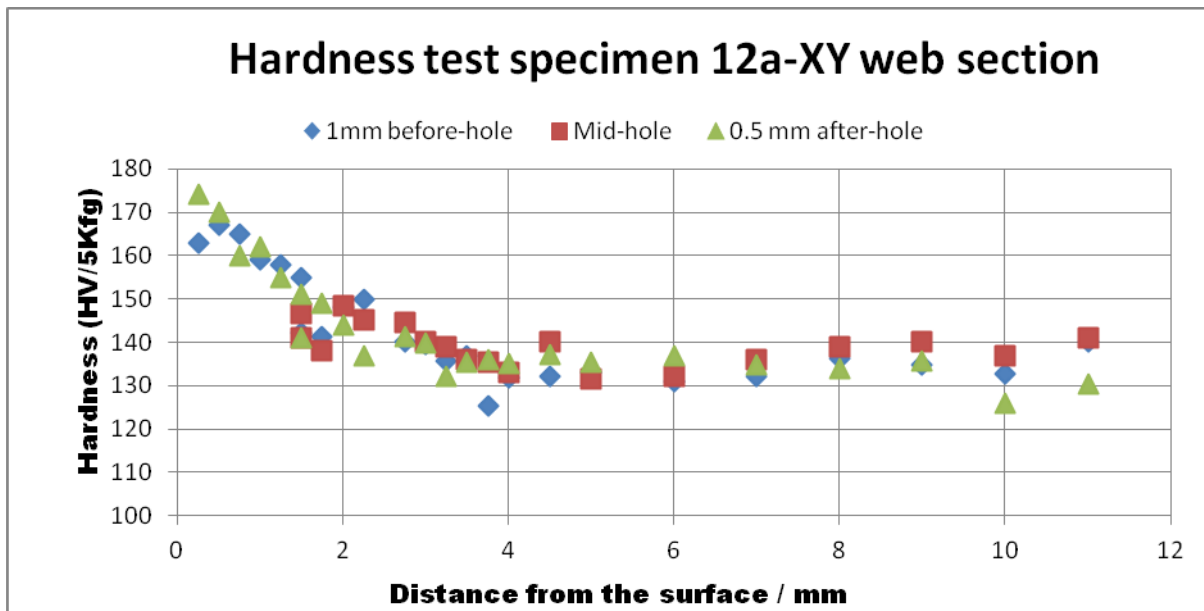


Figure 20: Result of hardness test on laser shock peened specimen 12a in the web section of Al 2099.

Maximum surface hardness value for specimen 12a is approximately 175 Hv. This value is because of laser shock peening effect. The depth of effect is approximately 2 mm. The unscattered hardness value outside the peening effect is 130 Hv while the scattered value is 135 Hv.

In summary, increase in hardness value achieved for sure with the peening for both specimens. The response is more on the web specimens as compare to the flange specimens.

The depth to which the peening penetrated the material was approximately 1.5 mm to 2 mm in the specimens in the flange and web sections of the extruded Al 2099. Due to a variation in

hardness values and depth penetration of specimens of the same sample at different locations, a suggestion is made here for further investigation. Preferably, by way of changing the peening parameters such as power density, number of layers and pulse duration to ascertain further variation in the hardness property of the specimens. (Fitzpatrick et al., 2015) reported a variation in surface residual stress profile reflected in hardness trend of Al 2624 when power density was varied from 1 to 7 shots as shown in figure 25.

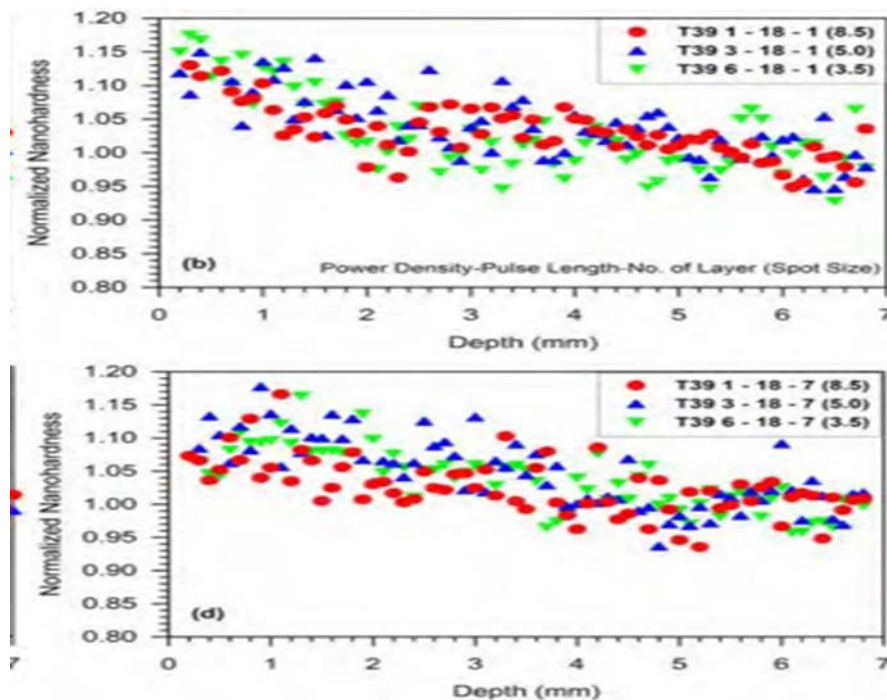


Figure 21: Variation in hardness trend due to power density change from 1 shot to 7 seven shots (Fitzpatrick et al., 2015).

Based on figure 25, peening parameters such as power density will create varying pulse profiles with varying hardening effects. This can be applied on Al 2099 to observe the hardness trend. Other peening parameters such as number of peened layers and duration can be varied on Al 2099 equally.

The change in the surface residual stress profile-reflected hardness response is likened to residual stress effect associated with power density and energy of Laser shock peening. So many literatures such as (Fitzpatrick et al., 2015), (khan et al, 2011) and (Sun et al., 2014) have pointed to that fact.

Different textures can also cause a variation in hardness and different textures respond differently to laser shock peening. For instance, the texture of the flange and the web in the same sample can vary. When texture varies, hardness varies too. When hardness varies, different responses should be expected from surface treatment techniques such as laser shock peening.

From the result in figure 26, the initial average hardness value of the flange was 140Hv while that of the web was 130 Hv. That was before laser shock peening was applied. After the

application of laser shock peening, the initial softer part (Web) showed a higher value of hardness value of up to 170 Hv. The flange which was initially harder than the web before laser shock peening showed a hardness increment value of up to 160Hv. By implication, it means the softer web developed more residual stress meaning better response to laser shock peening.

This result is also consistent with the report of various literatures on the positive effect of laser shock peening like (Sun et al., 2014), (Fu et al., 2014), (Hatamleh, 2007), (Hales & Hafley, 1998), (Sticchi et al., 2015), (Cuella et al, 2012), (King et al., 2006), (Hatamleh et al., 2007), (Nikitin et al., 2004) and (Fitzpatrick et al., 2015). This research is however specific on Al 2099.

Based on this correlation, this research confirms that laser shock peening improved the hardness of extruded Al 2099 by 18 % in the flange section and 21% in the web section.

Evidence hardness variation was reported by (Hales & Hafley, 1998) and (Fitzpatrick et al., 2015) as shown in figure 26.

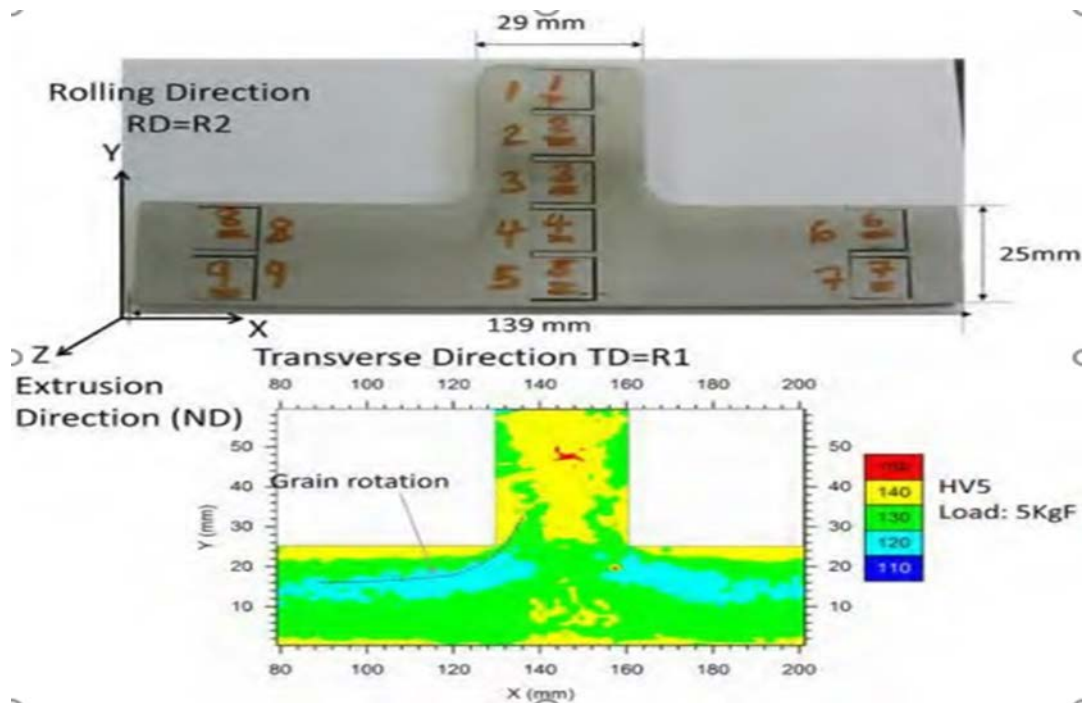


Figure 22: Unpeened bar of Al 2099 showing both axis and Vickers hardness variation (Fitzpatrick et al.: 2015).

(Singh & Jata, 2014) and (Denzer et al, 1992) explained further with evidence of varying texture in the flange and the web having (111), (200) and (220) textures as shown in figure 27.

The way crystallographic orientations are distributed in a polycrystalline sample is referred to as texture (Bunge, 2013). Or it can be said to be the preferred crystallographic orientation of a polycrystalline sample or simply, preferred crystallographic orientation.

Aluminium is compressed during hot extrusion in one direction. As it flows through the die under pressure, the crystals of aluminium deforms in the direction of extrusion. This grain

flow results in rolling texture. (Hirsch & Al-Samman, 2013) and (Sheppard, 2013).

Most materials pulled out in tension or compression have uniaxial or fibrous symmetry. Fibrous texture occurs because of symmetry rotation with respect to sample direction. Orientational transformation of crystals into one another takes place at equal frequency. Hence, rotationally symmetric textures are referred to as fibre textures (Newnham, 2005). It appears that the flange has rolling texture while the web has fibrous texture which may cause a variation in hardness response due to Laser Shock peening as reflected in the result in figures 27 to 29. While the partly fibrous texture responded to laser shock peening as reflected in figures 22 to 24.

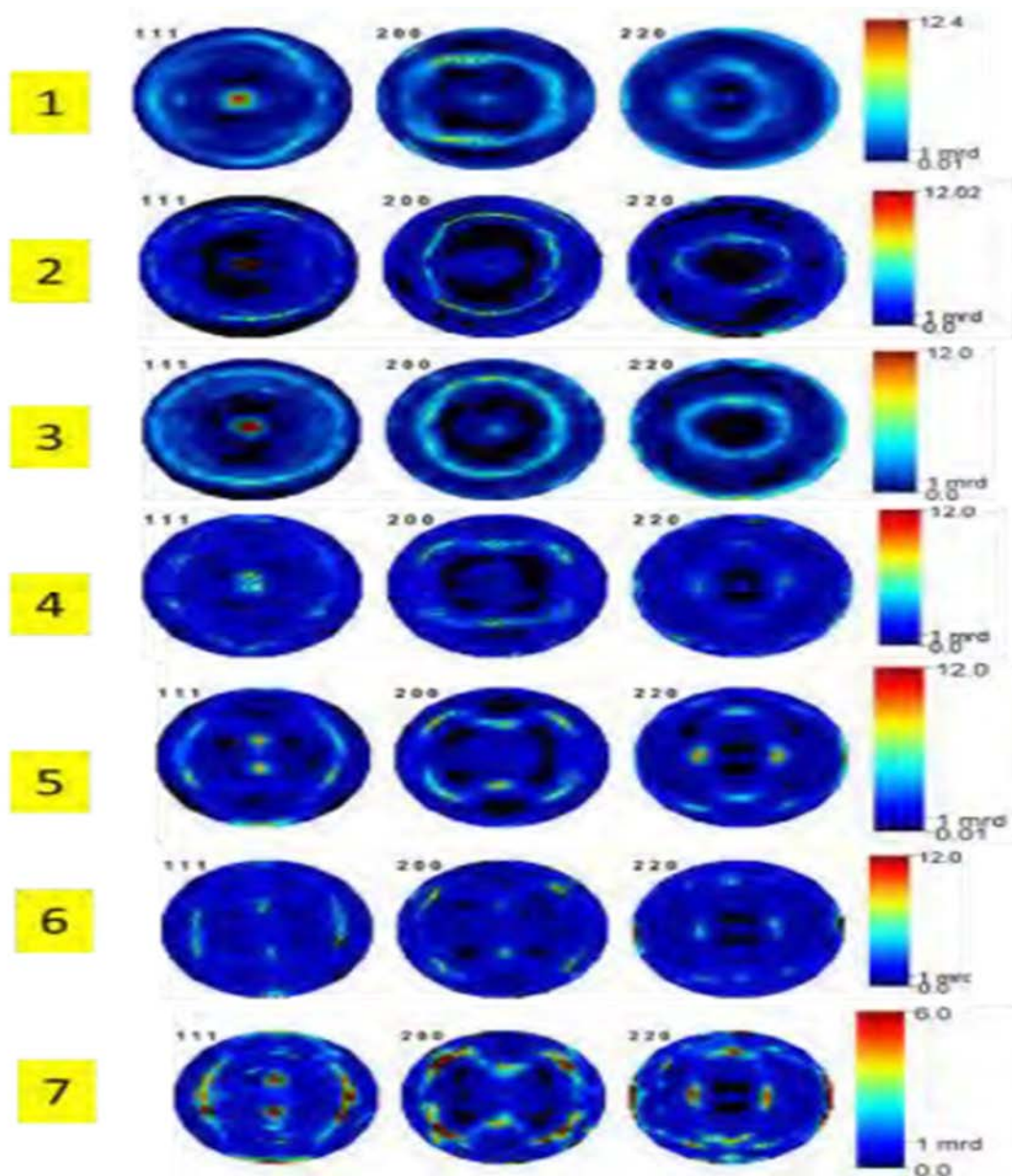


**Figure 23: Poles figures of extruded T bar present in the Flange and web of the Sample (Singh & Jata, 2014)**

In a separate study by (Sun et al, 2014) on Al 2196, improved mechanical properties such as surface hardness was achieved with mechanical shot peening. Multiple dimple like surface was observed after receiving multiple shots, as compared to the unpeened specimen. Mechanical properties improved at the detriment of smooth surface. Appearance of surface dimples due to mechanical shot peening phenomenon and local delamination was observed after shot peening. Due to the different speed of the shots, the craters were of average varying sizes of 100  $\mu\text{m}$  with irregular distribution on the surface. Overlap was caused by different impact of different shots resulting to the varying shapes and sizes of the craters. This is however a limitation of shot peening as the surface was damaged. This limitation has been overcome by laser Shock peening (Sticchi et al., 2015), (Cuella et al, 2012), (King et al., 2006), (Hatamleh et al., 2007), and (Nikitin et al., 2004). On the other hand, compressive residual stresses were generated on the

surface of the peened material. A value of -240.3 MPa was recorded at the surface. A maximum value of -265.5 MPa with 81  $\mu\text{m}$  was recorded. Uneven plastic deformation occurred at the surface of the Al 2196 Al-Li alloy producing compressive residual stresses that inhibit fatigue crack generation. This process resulted to increase in hardness in the surface region. Hardness test result showed a hardness value 201 HV at the surface with a decreasing inward hardness value to the average material matrix value of 146 HV. (Sun et al, 2014) achieved 37% increase in hardness value as compared to the unpeened specimen shown in figure 5.

## II. SUMMARY

This research has investigated the effect of Laser Shock Peening specifically on Al 2099 extruded. The magnitude of

response of the material to Laser shock peening is a function of the crystallographic texture and cyclic plasticity behaviour. Thermomechanical processing and heat treatment such as extrusion and laser shock peening influence crystallographic and plastic behaviour of Al 2099.

A variation in yield strength of the same material has been demonstrated. Hardening variation has been demonstrated too. The softer material in the web section tend to have more hardness response than the harder material in the flange after laser shock peened.

If the same material can possess different texture and cyclic plastic behaviour, care should be taken to categorise laser shock peening parameters per heat treatment, texture and cyclic plasticity behaviour. This is because different hardness response will mean different residual stresses.

Worthy of note is the fact that this research has been consistent with the expectation of different crystallographic textures at different locations in a hot extruded section due to temperate and local strain variations within that hot extruded cross section. Even though such expectations abound, until proven for each alloy as in the study. One cannot assume and conclude that different hardness and yield strength exist in the same material with complex geometry. Hence, the use of softwares with solvers such as finite element analysis and eigen strain analysis for modelling should bear in mind the assumption of such geometry as continuum and assumption of homogeneous material properties and assumption of homogeneous material properties.

### III. CONCLUSION

1. Al 2099 extruded T shaped possess different crystallographic textures at differing locations within the extruded cross section. This is reflected in the yield strength and hardness variation. There is evidence of fibrous texture in the web and rolling texture in the flange.

2. Inhomogeneous texture has influence on mechanical properties such as yield strength and hardness properties.

3. The softer part of the T bar of Extruded Al 2099 showed higher hardness response as compared to the harder part of the T bar.

4. Approximately 18 % and 21 % increment in maximum surface hardness was for the flange and web specimens respectively after treating them with Laser shock peening.

5. The cyclic behaviour of Al 2099 shows evidence of reverse yielding. This because the yield strength of all the specimens varied after the specimens were loaded and unloaded in cyclic manner. Even though due to the limitations of the Instron tensile testing machine, compressive part of loading cycles was not investigated to ascertain the specific values of  $\beta_{\sigma 1}$ ,  $\beta_{\sigma 2}$ , and  $\beta_{\sigma 3}$ .

### REFERENCES

[1] Bunge, H. (2013) *Texture Analysis in Materials Science: Mathematical Methods.*: Elsevier  
[2] Campbell Jr, F. C. (2011) *Manufacturing Technology for Aerospace Structural Materials.*: Elsevier

[3] Coratella, S., Burak Toparli, M., and Fitzpatrick, M. E. (eds.) (2014) *Materials Science Forum. 'Application of the Eigenstrain Theory to Predict Residual Stress Around Curved Edges After Laser Shock Peening'*: Trans Tech Publ  
[4] Cuellar, S. D., Hill, M. R., DeWald, A. T., and Rankin, J. E. (2012) 'Residual Stress and Fatigue Life in Laser Shock Peened Open Hole Samples'. *International Journal of Fatigue* 44, 8-13  
[5] Dursun, T. and Soutis, C. (2014) 'Recent Developments in Advanced Aircraft Aluminium Alloys'. *Materials & Design* 56, 862-871  
[6] Giummarra, C., Rioja, R., Bray, G., Magnusen, P., and Moran, J. (eds.) (2008) *Proc. ICAA11 Conference, Aachen, Germany. 'Al-Li Alloys: Development of Corrosion Resistant, High Toughness Aluminium-Lithium Aerospace Alloys'*  
[7] Liu, T., Wang, Y., Wu, J., Xia, X., Wang, J., Wang, W., and Wang, S. (2015) 'Springback Analysis of Z & T-Section 2196-T8511 and 2099-T83 Al-Li Alloys Extrusions in Displacement Controlled Cold Stretch Bending'. *Journal of Materials Processing Technology* 225, 295-309  
[8] Hales, S. and Hafley, R. (1998) 'Texture and Anisotropy in Al-Li Alloy 2195 Plate and Near-Net-Shape Extrusions'. *Materials Science and Engineering: A* 257 (1), 153-164  
[9] Hatamleh, O., Lyons, J., and Forman, R. (2007) 'Laser and Shot Peening Effects on Fatigue Crack Growth in Friction Stir Welded 7075-T7351 Aluminum Alloy Joints'. *International Journal of Fatigue* 29 (3), 421-434  
[10] HHirsch, J. and Al-Samman, T. (2013) 'Superior Light Metals by Texture Engineering: Optimized Aluminum and Magnesium Alloys for Automotive Applications'. *Acta Materialia* 61 (3), 818-843  
[11] Kalka, M. and Adamiec, J. (2006) 'Complex Procedure for the Quantitative Description of an Al-Si Cast Alloy Microstructure'. *Materials Characterization* 56 (4), 373-378  
[12] Karama, M. (2011) *Multi-Scales Behaviour of Materials Special Topic Volume with Invited Peer Reviewed Papers Only.* Zurich: Zurich : Trans Tech Publishers  
[13] Kaufman, J. G. (2000) *Introduction to Aluminum Alloys and Tempers.*: ASM international  
[14] King, A., Steuwer, A., Woodward, C., and Withers, P. (2006) 'Effects of Fatigue and Fretting on Residual Stresses Introduced by Laser Shock Peening'. *Materials Science and Engineering: A* 435, 12-18  
[15] Kissell, J. R. and Ferry, R. L. (2002) *Aluminum Structures: A Guide to their Specifications and Design.*: John Wiley & Sons  
[16] Meriç, C. (2000) 'Physical and Mechanical Properties of Cast Under Vacuum Aluminum Alloy 2024 Containing Lithium J. Lubliner, 2008Additions'. *Materials Research Bulletin* 35 (9), 1479-1494  
[17] Newnham, R. E. (2005) *Properties of Materials: Anisotropy, Symmetry, Structure.*: Oxford University Press on Demand  
[18] Nikitin, I., Scholtes, B., Maier, H., and Altenberger, I. (2004) 'High Temperature Fatigue Behavior and Residual Stress Stability of Laser-Shock Peened and Deep Rolled Austenitic Steel AISI 304'. *Scripta Materialia* 50 (10), 1345-1350  
[19] Prasad, N. E., Gokhale, A., and Wanhill, R. (2013) *Aluminum-Lithium Alloys: Processing, Properties, and Applications.* Butterworth-Heinemann  
[20] Sticchi, M., Schnubel, D., Kashaev, N., and Huber, N. (2015) 'Review of Residual Stress Modification Techniques for Extending the Fatigue Life of Metallic Aircraft Components'. *Applied Mechanics Reviews* 67 (1), 010801  
[21] Sun, B. L., Wang, Y. J., Xiao, J. Y., Gao, G. Q., Qiao, M. J., and Xiao, X. D. (2014) 'Evolution of Microstructure and Properties of 2196 Al-Li Alloy Induced by Shot Peening'. *Procedia Engineering* 81, 1043-1048  
[22] Wanhill, R. and Bray, G. (2013) 'Aerostructural Design and its Application to Aluminum-Lithium Alloys'. *Aluminum-Lithium Alloys: Processing, Properties, and Applications*, 27  
[23] Williams, J. C. and Starke, E. A. (2003) 'Progress in Structural Materials for Aerospace Systems'. *Acta Materialia* 51 (19), 5775-5799  
[24] Zabeen, S., Khan, M., and Fitzpatrick, M. (2015). *Mechanisms of Residual Stress Generation in Mechanical Surface Treatment: The Role of Cyclic Plasticity and Texture.*  
[25] Zhang, X., Zhang, Y., Lu, J., Xuan, F., Wang, Z., and Tu, S. (2010) 'Improvement of Fatigue Life of Ti-6Al-4V Alloy by Laser Shock Peening'. *Materials Science and Engineering: A* 527 (15), 3411-3415



AUTHORS

**First Author** – Jige, Felix Teryima, Department of Metalwork Technology, School of Technical Education, Federal College of Education (Technical), Potiskum., PMB 1013 Potiskum, Yobe state, Nigeria, jigefelixt@gmail.com, jiget@uni.coventry.ac.uk

**Second Author** – Peter Ali Malgwi, Metalwork Technology Department, School of Technical Education, FCE(T), Potiskum., Phone no: +2348084468661, pamalgwi@gmail.com  
**Third Author** – Mohammed Isa Bappa, Metalwork Technology Department, School of Technical Education, FCE(T), Potiskum. Phone no: +2347065689587, mohammedisabappa@gmail.com